Measurement of the Top-Quark Mass in All-Hadronic Decays in $p\bar{p}$ Collisions at CDF II

T. Aaltonen,[23] A. Abulencia,[24] J. Adelman,[13] T. Affolder,[10] T. Akimoto,[56] M.G. Albrow,[17] D. Ambrose,[17]
S. Amerio,[44] D. Amidei,[35] A. Anastassov,[53] K. Anikeev,[17] A. Annovi,[19] J. Antos,[14] M. Aoki,[56] G. Apollinari,[17]
J.-F. Arguin,[34] T. Arisawa,[58] A. Artikov,[15] W. Ashmanskas,[17] A. Attal,[8] F. Azfar,[43] P. Azzi-Bacchetta,[44]
P. Azzurri,[47] N. Bacchetta,[44] W. Badgett,[17] A. Barbaro-Galtieri,[29] V.E. Barnes,[49] B.A. Barnett,[25] S. Baroiant,[7]
V. Bartsch,[31] G. Bauer,[33] F. Bedeschi,[47] S. Behari,[25] S. Belforte,[55] G. Bellettini,[47] J. Bellinger,[60] A. Belloni,[33]
D. Benjamin,[16] A. Beretvas,[17] J. Beringer,[29] T. Berry,[30] A. Bhatti,[51] M. Binkley,[17] D. Bisello,[44] R.E. Blair,[2]
C. Blocker,[6] B. Blumenfeld,[25] A. Bocci,[16] A. Bodek,[50] V. Boisvert,[50] G. Bolla,[49] A. Bolshov,[33] D. Bortoletto,[49]
J. Boudreau,[48] A. Boveia,[10] B. Brau,[10] L. Brigliadori,[5] C. Bromberg,[36] E. Brubaker,[13] J. Budagov,[15] H.S. Budd,[50]
S. Budd,[24] S. Budroni,[47] K. Burkett,[17] G. Busetto,[44] P. Bussey,[21] K. L. Byrum,[2] S. Cabrera[o],[16] M. Campanelli,[20]
M. Campbell,[35] F. Canelli,[17] A. Canepa,[49] S. Carillo[i],[18] D. Carlsmith,[60] R. Carosi,[47] M. Casarsa,[55] A. Castro,[5]
P. Catastini,[47] D. Cauz,[55] M. Cavalli-Sforza,[3] A. Cerri,[29] L. Cerrito[m],[43] S.H. Chang,[28] Y.C. Chen,[1] M. Chertok,[7]
G. Chiarelli,[47] G. Chlachidze,[15] F. Chlebana,[17] I. Cho,[28] K. Cho,[28] D. Chokheli,[15] J.P. Chou,[22] G. Choudalakis,[33]
S.H. Chuang,[60] K. Chung,[12] W.H. Chung,[60] Y.S. Chung,[50] M. Ciljak,[47] C.I. Ciobanu,[24] M.A. Ciocci,[47] A. Clark,[20]
D. Clark,[6] M. Coca,[16] G. Compostella,[44] M.E. Convery,[51] J. Conway,[7] B. Cooper,[36] K. Copic,[35] M. Cordelli,[19]
G. Cortiana,[44] F. Crescioli,[47] C. Cuenca Almenar,[7] J. Cuevas[l],[11] R. Culbertson,[17] J.C. Cully,[35] D. Cyr,[60]
S. DaRonco,[44] M. Datta,[17] S. D'Auria,[21] T. Davies,[21] M. D'Onofrio,[3] D. Dagenhart,[6] P. de Barbaro,[50]
S. De Cecco,[52] A. Deisher,[29] G. De Lentdecker[c],[50] M. Dell'Orso,[47] F. Delli Paoli,[44] L. Demortier,[51] J. Deng,[16]
M. Deninno,[5] D. De Pedis,[52] P.F. Derwent,[17] G.P. Di Giovanni,[45] C. Dionisi,[52] B. Di Ruzza,[55] J.R. Dittmann,[4]
P. DiTuro,[53] C. Dörr,[26] S. Donati,[47] M. Donega,[20] P. Dong,[8] J. Donini,[44] T. Dorigo,[44] S. Dube,[53] J. Efron,[40]
R. Erbacher,[7] D. Errede,[24] S. Errede,[24] R. Eusebi,[17] H.C. Fang,[29] S. Farrington,[30] I. Fedorko,[47] W.T. Fedorko,[13]
R.G. Feild,[61] M. Feindt,[26] J.P. Fernandez,[32] R. Field,[18] G. Flanagan,[49] A. Foland,[22] S. Forrester,[7] G.W. Foster,[17]
M. Franklin,[22] J.C. Freeman,[29] I. Furic,[13] M. Gallinaro,[51] J. Galyardt,[12] J.E. Garcia,[47] F. Garberson,[10]
A.F. Garfinkel,[49] C. Gay,[61] H. Gerberich,[24] D. Gerdes,[35] S. Giagu,[52] P. Giannetti,[47] A. Gibson,[29] K. Gibson,[48]
J.L. Gimmell,[50] C. Ginsburg,[17] N. Giokaris[a],[15] M. Giordani,[55] P. Giromini,[19] M. Giunta,[47] G. Giurgiu,[12]
V. Glagolev,[15] D. Glenzinski,[17] M. Gold,[38] N. Goldschmidt,[18] J. Goldstein[b],[43] A. Golossanov,[17] G. Gomez,[11]
G. Gomez-Ceballos,[11] M. Goncharov,[54] O. González,[32] I. Gorelov,[38] A.T. Goshaw,[16] K. Goulianos,[51] A. Gresele,[44]
M. Griffiths,[30] S. Grinstein,[22] C. Grosso-Pilcher,[13] R.C. Group,[18] U. Grundler,[24] J. Guimaraes da Costa,[22]
Z. Gunay-Unalan,[36] C. Haber,[29] K. Hahn,[33] S.R. Hahn,[17] E. Halkiadakis,[53] A. Hamilton,[34] B.-Y. Han,[50]
J.Y. Han,[50] R. Handler,[60] F. Happacher,[19] K. Hara,[56] M. Hare,[57] S. Harper,[43] R.F. Harr,[59] R.M. Harris,[17]
M. Hartz,[48] K. Hatakeyama,[51] J. Hauser,[8] A. Heijboer,[46] B. Heinemann,[30] J. Heinrich,[46] C. Henderson,[33]
M. Herndon,[60] J. Heuser,[26] D. Hidas,[16] C.S. Hill[b],[10] D. Hirschbuehl,[26] A. Hocker,[17] A. Holloway,[22] S. Hou,[1]
M. Houlden,[30] S.-C. Hsu,[9] B.T. Huffman,[43] R.E. Hughes,[40] U. Husemann,[61] J. Huston,[36] J. Incandela,[10]
G. Introzzi,[47] M. Iori,[52] Y. Ishizawa,[56] A. Ivanov,[7] B. Iyutin,[33] E. James,[17] D. Jang,[53] B. Jayatilaka,[35] D. Jeans,[52]
H. Jensen,[17] E.J. Jeon,[28] S. Jindariani,[18] M. Jones,[49] K.K. Joo,[28] S.Y. Jun,[12] J.E. Jung,[28] T.R. Junk,[24]
T. Kamon,[54] P.E. Karchin,[59] Y. Kato,[42] Y. Kemp,[26] R. Kephart,[17] U. Kerzel,[26] V. Khotilovich,[54]
B. Kilminster,[40] D.H. Kim,[28] H.S. Kim,[28] J.E. Kim,[28] M.J. Kim,[12] S.B. Kim,[28] S.H. Kim,[56] Y.K. Kim,[13]
N. Kimura,[56] L. Kirsch,[6] S. Klimenko,[18] M. Klute,[33] B. Knuteson,[33] B.R. Ko,[16] K. Kondo,[58] D.J. Kong,[28]
J. Konigsberg,[18] A. Korytov,[18] A.V. Kotwal,[16] A. Kovalev,[46] A.C. Kraan,[46] J. Kraus,[24] I. Kravchenko,[33]
M. Kreps,[26] J. Kroll,[46] N. Krumnack,[4] M. Kruse,[16] V. Krutelyov,[10] T. Kubo,[56] S. E. Kuhlmann,[2] T. Kuhr,[26]
Y. Kusakabe,[58] S. Kwang,[13] A.T. Laasanen,[49] S. Lai,[34] S. Lami,[47] S. Lammel,[17] M. Lancaster,[31] R.L. Lander,[7]
K. Lannon,[40] A. Lath,[53] G. Latino,[47] I. Lazzizzera,[44] T. LeCompte,[2] J. Lee,[50] J. Lee,[28] Y.J. Lee,[28] S.W. Lee[n],[54]
R. Lefèvre,[3] N. Leonardo,[33] S. Leone,[47] S. Levy,[13] J.D. Lewis,[17] C. Lin,[61] C.S. Lin,[17] M. Lindgren,[17] E. Lipeles,[9]
A. Lister,[7] D.O. Litvintsev,[17] T. Liu,[17] N.S. Lockyer,[46] A. Loginov,[61] M. Loreti,[44] P. Loverre,[52] R.-S. Lu,[1]
D. Lucchesi,[44] P. Lujan,[29] P. Lukens,[17] G. Lungu,[18] L. Lyons,[43] J. Lys,[29] R. Lysak,[14] E. Lytken,[49] P. Mack,[26]
D. MacQueen,[34] R. Madrak,[17] K. Maeshima,[17] K. Makhoul,[33] T. Maki,[23] P. Maksimovic,[25] S. Malde,[43] G. Manca,[30]
F. Margaroli,[5] R. Marginean,[17] C. Marino,[26] C.P. Marino,[24] A. Martin,[61] M. Martin,[21] V. Martin[g],[21] M. Martínez,[3]
T. Maruyama,[56] P. Mastrandrea,[52] T. Masubuchi,[56] H. Matsunaga,[56] M.E. Mattson,[59] R. Mazini,[34] P. Mazzanti,[5]
K.S. McFarland,[50] P. McIntyre,[54] R. McNulty[f],[30] A. Mehta,[30] P. Mehtala,[23] S. Menzemer[h],[11] A. Menzione,[47]

P. Merkel,[49] C. Mesropian,[51] A. Messina,[36] T. Miao,[17] N. Miladinovic,[6] J. Miles,[33] R. Miller,[36] C. Mills,[10]
M. Milnik,[26] A. Mitra,[1] G. Mitselmakher,[18] A. Miyamoto,[27] S. Moed,[20] N. Moggi,[5] B. Mohr,[8] R. Moore,[17]
M. Morello,[47] P. Movilla Fernandez,[29] J. Mülmenstädt,[29] A. Mukherjee,[17] Th. Muller,[26] R. Mumford,[25]
P. Murat,[17] J. Nachtman,[17] A. Nagano,[56] J. Naganoma,[58] I. Nakano,[41] A. Napier,[57] V. Necula,[18] C. Neu,[46]
M.S. Neubauer,[9] J. Nielsen,[29] T. Nigmanov,[48] L. Nodulman,[2] O. Norniella,[3] E. Nurse,[31] S.H. Oh,[16] Y.D. Oh,[28]
I. Oksuzian,[18] T. Okusawa,[42] R. Oldeman,[30] R. Orava,[23] K. Osterberg,[23] C. Pagliarone,[47] E. Palencia,[11]
V. Papadimitriou,[17] A.A. Paramonov,[13] B. Parks,[40] S. Pashapour,[34] J. Patrick,[17] G. Pauletta,[55] M. Paulini,[12]
C. Paus,[33] D.E. Pellett,[7] A. Penzo,[55] T.J. Phillips,[16] G. Piacentino,[47] J. Piedra,[45] L. Pinera,[18] K. Pitts,[24]
C. Plager,[8] L. Pondrom,[60] X. Portell,[3] O. Poukhov,[15] N. Pounder,[43] F. Prakoshyn,[15] A. Pronko,[17] J. Proudfoot,[2]
F. Ptohos[e],[19] G. Punzi,[47] J. Pursley,[25] J. Rademacker[b],[43] A. Rahaman,[48] N. Ranjan,[49] S. Rappoccio,[22]
B. Reisert,[17] V. Rekovic,[38] P. Renton,[43] M. Rescigno,[52] S. Richter,[26] F. Rimondi,[5] L. Ristori,[47] A. Robson,[21]
T. Rodrigo,[11] E. Rogers,[24] S. Rolli,[57] R. Roser,[17] M. Rossi,[55] R. Rossin,[18] A. Ruiz,[11] J. Russ,[12] V. Rusu,[13]
H. Saarikko,[23] S. Sabik,[34] A. Safonov,[54] W.K. Sakumoto,[50] G. Salamanna,[52] O. Saltó,[3] D. Saltzberg,[8] C. Sánchez,[3]
L. Santi,[55] S. Sarkar,[52] L. Sartori,[47] K. Sato,[17] P. Savard,[34] A. Savoy-Navarro,[45] T. Scheidle,[26] P. Schlabach,[17]
E.E. Schmidt,[17] M.P. Schmidt,[61] M. Schmitt,[39] T. Schwarz,[7] L. Scodellaro,[11] A.L. Scott,[10] A. Scribano,[47]
F. Scuri,[47] A. Sedov,[49] S. Seidel,[38] Y. Seiya,[42] A. Semenov,[15] L. Sexton-Kennedy,[17] A. Sfyrla,[20] M.D. Shapiro,[29]
T. Shears,[30] P.F. Shepard,[48] D. Sherman,[22] M. Shimojima[k],[56] M. Shochet,[13] Y. Shon,[60] I. Shreyber,[37] A. Sidoti,[47]
P. Sinervo,[34] A. Sisakyan,[15] J. Sjolin,[43] A.J. Slaughter,[17] J. Slaunwhite,[40] K. Sliwa,[57] J.R. Smith,[7] F.D. Snider,[17]
R. Snihur,[34] M. Soderberg,[35] A. Soha,[7] S. Somalwar,[53] V. Sorin,[36] J. Spalding,[17] F. Spinella,[47] T. Spreitzer,[34]
P. Squillacioti,[47] M. Stanitzki,[61] A. Staveris-Polykalas,[47] R. St. Denis,[21] B. Stelzer,[8] O. Stelzer-Chilton,[43]
D. Stentz,[39] J. Strologas,[38] D. Stuart,[10] J.S. Suh,[28] A. Sukhanov,[18] H. Sun,[57] T. Suzuki,[56] A. Taffard,[24]
R. Takashima,[41] Y. Takeuchi,[56] K. Takikawa,[56] M. Tanaka,[2] R. Tanaka,[41] M. Tecchio,[35] P.K. Teng,[1] K. Terashi,[51]
J. Thom[d],[17] A.S. Thompson,[21] E. Thomson,[46] P. Tipton,[61] V. Tiwari,[12] S. Tkaczyk,[17] D. Toback,[54] S. Tokar,[14]
K. Tollefson,[36] T. Tomura,[56] D. Tonelli,[47] S. Torre,[19] D. Torretta,[17] S. Tourneur,[45] W. Trischuk,[34] R. Tsuchiya,[58]
S. Tsuno,[41] N. Turini,[47] F. Ukegawa,[56] T. Unverhau,[21] S. Uozumi,[56] D. Usynin,[46] S. Vallecorsa,[20]
N. van Remortel,[23] A. Varganov,[35] E. Vataga,[38] F. Vázquez[i],[18] G. Velev,[17] G. Veramendi,[24] V. Veszpremi,[49]
R. Vidal,[17] I. Vila,[11] R. Vilar,[11] T. Vine,[31] I. Vollrath,[34] I. Volobouev[n],[29] G. Volpi,[47] F. Würthwein,[9] P. Wagner,[54]
R.G. Wagner,[2] R.L. Wagner,[17] J. Wagner,[26] W. Wagner,[26] R. Wallny,[8] S.M. Wang,[1] A. Warburton,[34]
S. Waschke,[21] D. Waters,[31] W.C. Wester III,[17] B. Whitehouse,[57] D. Whiteson,[46] A.B. Wicklund,[2]
E. Wicklund,[17] G. Williams,[34] H.H. Williams,[46] P. Wilson,[17] B.L. Winer,[40] P. Wittich[d],[17] S. Wolbers,[17]
C. Wolfe,[13] T. Wright,[35] X. Wu,[20] S.M. Wynne,[30] A. Yagil,[17] K. Yamamoto,[42] J. Yamaoka,[53] T. Yamashita,[41]
C. Yang,[61] U.K. Yang[j],[13] Y.C. Yang,[28] W.M. Yao,[29] G.P. Yeh,[17] J. Yoh,[17] K. Yorita,[13] T. Yoshida,[42] G.B. Yu,[50]
I. Yu,[28] S.S. Yu,[17] J.C. Yun,[17] L. Zanello,[52] A. Zanetti,[55] I. Zaw,[22] X. Zhang,[24] J. Zhou,[53] and S. Zucchelli[5]
(CDF Collaboration*)

[1]*Institute of Physics, Academia Sinica, Taipei, Taiwan 11529, Republic of China*
[2]*Argonne National Laboratory, Argonne, Illinois 60439*
[3]*Institut de Fisica d'Altes Energies, Universitat Autonoma de Barcelona, E-08193, Bellaterra (Barcelona), Spain*
[4]*Baylor University, Waco, Texas 76798*
[5]*Istituto Nazionale di Fisica Nucleare, University of Bologna, I-40127 Bologna, Italy*
[6]*Brandeis University, Waltham, Massachusetts 02254*
[7]*University of California, Davis, Davis, California 95616*
[8]*University of California, Los Angeles, Los Angeles, California 90024*
[9]*University of California, San Diego, La Jolla, California 92093*
[10]*University of California, Santa Barbara, Santa Barbara, California 93106*
[11]*Instituto de Fisica de Cantabria, CSIC-University of Cantabria, 39005 Santander, Spain*
[12]*Carnegie Mellon University, Pittsburgh, PA 15213*
[13]*Enrico Fermi Institute, University of Chicago, Chicago, Illinois 60637*
[14]*Comenius University, 842 48 Bratislava, Slovakia; Institute of Experimental Physics, 040 01 Kosice, Slovakia*
[15]*Joint Institute for Nuclear Research, RU-141980 Dubna, Russia*
[16]*Duke University, Durham, North Carolina 27708*
[17]*Fermi National Accelerator Laboratory, Batavia, Illinois 60510*
[18]*University of Florida, Gainesville, Florida 32611*
[19]*Laboratori Nazionali di Frascati, Istituto Nazionale di Fisica Nucleare, I-00044 Frascati, Italy*
[20]*University of Geneva, CH-1211 Geneva 4, Switzerland*
[21]*Glasgow University, Glasgow G12 8QQ, United Kingdom*

[22]*Harvard University, Cambridge, Massachusetts 02138*
[23]*Division of High Energy Physics, Department of Physics,*
University of Helsinki and Helsinki Institute of Physics, FIN-00014, Helsinki, Finland
[24]*University of Illinois, Urbana, Illinois 61801*
[25]*The Johns Hopkins University, Baltimore, Maryland 21218*
[26]*Institut für Experimentelle Kernphysik, Universität Karlsruhe, 76128 Karlsruhe, Germany*
[27]*High Energy Accelerator Research Organization (KEK), Tsukuba, Ibaraki 305, Japan*
[28]*Center for High Energy Physics: Kyungpook National University,*
Taegu 702-701, Korea; Seoul National University, Seoul 151-742,
Korea; and SungKyunKwan University, Suwon 440-746, Korea
[29]*Ernest Orlando Lawrence Berkeley National Laboratory, Berkeley, California 94720*
[30]*University of Liverpool, Liverpool L69 7ZE, United Kingdom*
[31]*University College London, London WC1E 6BT, United Kingdom*
[32]*Centro de Investigaciones Energeticas Medioambientales y Tecnologicas, E-28040 Madrid, Spain*
[33]*Massachusetts Institute of Technology, Cambridge, Massachusetts 02139*
[34]*Institute of Particle Physics: McGill University, Montréal,*
Canada H3A 2T8; and University of Toronto, Toronto, Canada M5S 1A7
[35]*University of Michigan, Ann Arbor, Michigan 48109*
[36]*Michigan State University, East Lansing, Michigan 48824*
[37]*Institution for Theoretical and Experimental Physics, ITEP, Moscow 117259, Russia*
[38]*University of New Mexico, Albuquerque, New Mexico 87131*
[39]*Northwestern University, Evanston, Illinois 60208*
[40]*The Ohio State University, Columbus, Ohio 43210*
[41]*Okayama University, Okayama 700-8530, Japan*
[42]*Osaka City University, Osaka 588, Japan*
[43]*University of Oxford, Oxford OX1 3RH, United Kingdom*
[44]*University of Padova, Istituto Nazionale di Fisica Nucleare,*
Sezione di Padova-Trento, I-35131 Padova, Italy
[45]*LPNHE, Universite Pierre et Marie Curie/IN2P3-CNRS, UMR7585, Paris, F-75252 France*
[46]*University of Pennsylvania, Philadelphia, Pennsylvania 19104*
[47]*Istituto Nazionale di Fisica Nucleare Pisa, Universities of Pisa,*
Siena and Scuola Normale Superiore, I-56127 Pisa, Italy
[48]*University of Pittsburgh, Pittsburgh, Pennsylvania 15260*
[49]*Purdue University, West Lafayette, Indiana 47907*
[50]*University of Rochester, Rochester, New York 14627*
[51]*The Rockefeller University, New York, New York 10021*
[52]*Istituto Nazionale di Fisica Nucleare, Sezione di Roma 1,*
University of Rome "La Sapienza," I-00185 Roma, Italy
[53]*Rutgers University, Piscataway, New Jersey 08855*
[54]*Texas A&M University, College Station, Texas 77843*
[55]*Istituto Nazionale di Fisica Nucleare, University of Trieste/ Udine, Italy*
[56]*University of Tsukuba, Tsukuba, Ibaraki 305, Japan*
[57]*Tufts University, Medford, Massachusetts 02155*
[58]*Waseda University, Tokyo 169, Japan*
[59]*Wayne State University, Detroit, Michigan 48201*
[60]*University of Wisconsin, Madison, Wisconsin 53706*
[61]*Yale University, New Haven, Connecticut 06520*

(Dated: December 7, 2006)

We present a measurement of the top-quark mass, $M_{\rm top}$, in the all-hadronic decay channel $t\bar{t} \rightarrow W^+bW^-\bar{b} \rightarrow q_1\bar{q}_2bq_3\bar{q}_4\bar{b}$. The analysis is performed using 310 pb^{-1} of $\sqrt{s}$=1.96 TeV $p\bar{p}$ collisions collected with the CDF II detector using a multi-jet trigger. The mass measurement is based on an event-by-event likelihood which depends on both the sample purity and the value of the top-quark mass, using 90 possible jet-to-parton assignments in the six-jet final state. The joint likelihood of 290 selected events yields a value of $M_{\rm top}$=177.1 ± 4.9 (stat.) ± 4.7 (syst.) GeV/c^2.

PACS numbers: 14.65.Ha, 12.15.Ff

---

*With visitors from [a]University of Athens, [b]University of Bristol, [c]University Libre de Bruxelles, [d]Cornell University, [e]University of Cyprus, [f]University of Dublin, [g]University of

The mass of the top quark, $M_{\rm top}$, is an important free parameter of the standard model (SM) and is of the order of the electroweak symmetry breaking scale. Since virtual top quarks are involved in higher-order electroweak processes, by measuring the top-quark mass one can constrain the mass of the SM Higgs boson [1] and particles predicted in extensions of the SM [2]. At the Tevatron, $t\bar{t}$ pairs are produced by QCD processes and decay according to the CKM matrix [3] with a branching ratio of almost 100% into a W boson and a b quark. The final state of the event is then defined by the decay of the W bosons. All-hadronic $t\bar{t}$ events, where both of the W bosons decay into quarks, have a multi-jet final state and no missing energy due to neutrinos. The top-quark mass measurement in this decay channel is motivated by the large branching fraction (≈44%) and the complete reconstruction of both top and antitop quarks, relying only on hadronic jets. It is the first top-quark mass measurement in this channel using Tevatron Run II data, and serves as a consistency check of the measurements in the two other $t\bar{t}$ decay modes [4, 5]. The major experimental challenge is the presence of a large amount of multi-jet background events from QCD processes, which dominates $t\bar{t}$ production by three orders of magnitude, even after applying a trigger dedicated to events with a multi-jet final state.

In this Letter, we present the measurement of the top-quark mass in the all-hadronic decay channel using a sample of $t\bar{t}$ decays corresponding to 310 pb^{-1} of proton-antiproton collisions at $\sqrt{s}$=1.96 TeV, collected using the CDF II detector between February, 2002, and August, 2004. We measure the mass using the ideogram method, which was used in the DELPHI experiment at LEP for the W boson mass measurement [6]. The method is based on an event-by-event likelihood that reconstructs the top and antitop quarks using all 90 assignments of jets to quarks from W boson decays and b quarks (jet combinations) from the $t\bar{t}$ decay. Considering all jet combinations enhances the amount of top-quark mass information we can extract from each event. The 90 jet combinations arise from the 6!/8 permutations of the six jets, where the two possible top antitop permutations and the two possible permutations of each of the two quark pairs coming from the W decay are treated equally.

The sample purity, $\mathcal{P}$, defined as the fraction of all-hadronic $t\bar{t}$ events contained in the selected data sample, is a free parameter of the likelihood together with the value of $M_{\rm top}$. The reason for measuring both $M_{\rm top}$ and $\mathcal{P}$ simultaneously is that the cross sections of the QCD backgrounds are not well known. Even though the background processes do not contain any the top-quark mass information, the sensitivity of the likelihood on $M_{\rm top}$ does depend on the total amount of QCD background events. This is reflected both in the statistical variance of $M_{\rm top}$, and in corrections applied to $M_{\rm top}$ which take into account the presence of background events.

The CDF II detector [7] is a general-purpose charged and neutral particle detector designed to study $p\bar{p}$ collisions at the Fermilab Tevatron. It consists of an eight-layer silicon microstrip detector array and a cylindrical drift chamber contained inside a 1.4-T solenoid magnet, surrounded by electromagnetic and hadronic sampling calorimeters with a geometrical acceptance up to a pseudorapidity of $|\eta| = 3.6$ [8]. Muon chambers are located outside the calorimeters, allowing the reconstruction of track segments for penetrating particles.

The dataset used for this measurement is selected with a multi-jet trigger that relies solely on calorimetry. This trigger requires at least four calorimeter clusters with a transverse energy $E_{\rm T} > 15$ GeV and the scalar sum of the transverse jet energies to exceed 125 GeV. To improve the signal-to-background ratio, we impose offline kinematic requirements based on the scalar sum of the transverse jet energies and event shape observables. A full description of the trigger and kinematic selection is given in an earlier publication [9]. For the final top-quark mass measurement we consider only events with exactly six jets, each with transverse energy $E_{\rm T} > 15$ GeV and pseudorapidity $|\eta| \leq 2$. Jets are identified as clusters of energy deposits in the calorimeter segments (towers) which fall within a cone radius of $\Delta R = \sqrt{\Delta\phi^2 + \Delta\eta^2} \leq 0.4$ [8]. The raw jet energy scale (JES) is the result of a multi-step correction procedure to convert the measured transverse jet energy to the expected transverse energy of the parton corresponding to the jet. The corrections, assessed using data and a simulation of the CDF detector, include corrections for the response inhomogeneity in η, contributions from multiple interactions, the non-linearity of the calorimeter response, the underlying event, and the energy flow out of the jet cone [10]. We apply additional jet-parton energy corrections, specific to $t\bar{t}$ events, which are parameterized independently for b-quark jets and light-flavor jets [11].

In order to further reduce the QCD background, we apply b-quark identification to each event passing the kinematic selection. At least one jet must have a reconstructed displaced vertex (b-tag), consistent with a long-lived bottom hadron [12]. This displaced vertex information is not used to reduce the number of jet combinations in the event likelihood. Instead, we derive a weight factor using the CDF jet probability algorithm [13] which takes into account the probability that a jet originates from a b quark, as explained below. The final data sample contains 290 events. Assuming a theoretical cross section of 6.1 pb [14] for a top-quark mass of 178 GeV/c^2 [15], the

---

Edinburgh, [h]University of Heidelberg, [i]Universidad Iberoamericana, [j]University of Manchester, [k]Nagasaki Institute of Applied Science, [l]University de Oviedo, [m]University of London, Queen Mary and Westfield College, [n]Texas Tech University, [o]IFIC(CSIC-Universitat de Valencia),

expected signal-to-background ratio is about one-to-five.

By applying energy and momentum conservation we fit the momenta of the jets and the two top-quark masses, $m_i^{1,2}$, and determine their estimated uncertainties, $\sigma_i^{1,2}$ using a χ^2 minimization. This kinematic fit is applied to each of the 90 jet combinations, i, where we constrain the masses of the two W bosons to a world average value of $m_W = 80.4\ \mathrm{GeV}/c^2$ [3] within their natural widths. In order to achieve a better background reduction, the two reconstructed top-quark masses, $m_i^{1,2}$, are not constrained to be equal. The $m_i^{1,2}$ distributions thus obtained peak around 160 GeV/c^2 and range from 100–300 GeV/c^2 for the whole data sample, while the uncertainties $\sigma_i^{1,2}$ are typically of the order of 15 GeV/c^2 and range from 5–30 GeV/c^2. We measure M_{top} using an event likelihood where we weigh each combination i with a factor w_i, expressing the compatibility with both the $t\bar{t}$ decay kinematics and the presence of two b-quark jets together with four light-flavor jets. The weight factor w_i is calculated as

$$w_i = \exp\left(-\frac{1}{2}\chi_i^2\right) w_i^b, \tag{1}$$

where the exponential term, calculated using the χ^2 value of the kinematic fit, is a measure of the compatibility of jet combination i with the kinematics of a decaying $t\bar{t}$ pair. The second factor, w_i^b, gives the probability of two of the jets to originate from a b (or $\bar{b}$) quark and four others to originate from light quarks (including c quarks), and is given by

$$w_i^b = \prod_{j=1}^{2} p_j^b \prod_{j=3}^{6} p_j^q, \tag{2}$$

where we assume quarks with indices 3-6 to be light quarks originating from the W bosons. The probability $p_j^{b(\mathrm{or}\ q)}$ for a jet j to originate from a b quark (or light-flavor quark, q) is obtained using the CDF jet probability algorithm [13]. This calculates the probability P_j for a given jet j to originate from the primary vertex, based on the impact parameter information from the tracks belonging to that jet. The P_j distribution for b-quark jets (or light-flavor jets) is described by a probability density function, $f(b(\mathrm{or}\ q)|P_j)$ in order to obtain

$$p_j^{b(\mathrm{or}\ q)} = \frac{f(b(\mathrm{or}\ q)|P_j)}{f(b|P_j) + f(q|P_j)}. \tag{3}$$

The event likelihood consists of two terms. The signal likelihood term corresponds to the convolution of two Breit-Wigner distributions, $F_{\mathrm{BW}}(m'_j|M_{\mathrm{top}})$, with two Gaussians, $G(m'_j|m_i^j, \sigma_i^j)$, describing the experimental resolutions, $\sigma_i^{1,2}$, for each of the two reconstructed top-quark masses, $m_i^{1,2}$:

$$\mathcal{L}_i^{\mathrm{sig}}(M_{\mathrm{top}}) = \prod_{j=1,2} \int G(m'_j|m_i^j, \sigma_i^j) \times F_{\mathrm{BW}}(m'_j|M_{\mathrm{top}}) \mathrm{d}m'_j. \tag{4}$$

The M_{top}-independent background likelihood term, $\mathcal{L}_i^{\mathrm{bg}}$, corresponds to the two-dimensional posteriori probability density function (histogram) of $m_i^{1,2}$ obtained from ALPGEN [16] Monte Carlo (MC) multi-jet QCD background. All MC events are passed through the CDF detector simulation and are subjected to the same event selection criteria as the data.

The likelihood for a given event n is derived by summing the signal and background event likelihoods for each jet combination i and is calculated as a function of the top-quark mass, M_{top}, and the sample purity, $\mathcal{P}$:

$$\mathcal{L}^n(M_{\mathrm{top}}, \mathcal{P}) = \sum_{i=1}^{90} w_i \left[\mathcal{P}\mathcal{L}_i^{\mathrm{sig}}(M_{\mathrm{top}}) + (1-\mathcal{P})\mathcal{L}_i^{\mathrm{bg}}\right]. \tag{5}$$

We obtain a one-dimensional likelihood curve as a function of M_{top} by maximizing the two-dimensional joint likelihood,

$$L(M_{\mathrm{top}}, \mathcal{P}) = \prod_{n=1}^{290} \mathcal{L}^n(M_{\mathrm{top}}, \mathcal{P}), \tag{6}$$

with respect to the sample purity, $\mathcal{P}$, for each value of M_{top}. The maximum of the total likelihood of the 290 selected data events corresponds to a sample purity value of $\mathcal{P} = 0.21 \pm 0.07(\mathrm{stat.})$, which is compatible with a signal-to-background ratio of about one-to-five expected from SM $t\bar{t}$ production. The value of M_{top} extracted from the joint likelihood fit in Eq. (6) is biased due to the presence of wrong jet combinations, background events,

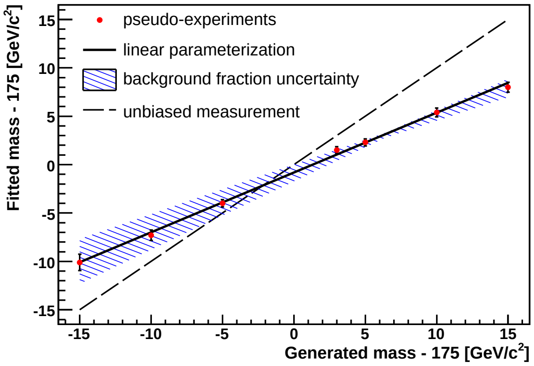

FIG. 1: The correlation between the measured value of M_{top} and the generated top-quark mass obtained with pseudo-experiments using $t\bar{t}$ signal events generated with HERWIG and an admixture of QCD background generated with ALPGEN. The solid line represents the linear parameterization used to correct M_{top}. The shaded band shows the effect of a one-sigma variation of the sample purity, $\mathcal{P} = 0.21 \pm 0.07(\mathrm{stat.})$. The dashed line corresponds to 100% correlation and zero offset.

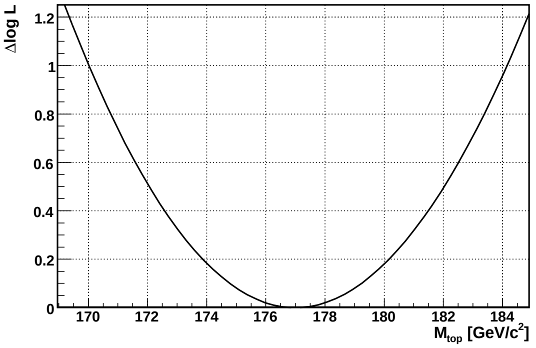

FIG. 2: The one-dimensional negative log-likelihood of $M_{\rm top}$ obtained including corrections using the parameterization shown in Fig. 1

and assignment of jets that arise from initial- (ISR) and final-state gluon radiation (FSR). Therefore, we correct the measurement of $M_{\rm top}$ using a linear parameterization of the correlation between the generated top-quark mass value and the mass estimator $M_{\rm top}$ in the range between 160 GeV/c^2 and 190 GeV/c^2, as shown in Fig. 1. Each mass point is obtained from pseudo-experiments with MC samples containing a mixture of 290 Poisson-fluctuated signal plus background events. We use HERWIG [17] to generate the $t\bar{t}$ signal events and ALPGEN to model the QCD background. The tag rate matrix used in [9] models the false identification of b-quarks. The correction depends on the sample purity used to construct the pseudo-experiments as illustrated by the shaded band which corresponds to the one-sigma statistical uncertainty on the sample purity measured from data. Accordingly, we assign a systematic uncertainty due to this purity uncertainty. Using the same pseudo-experiments we verify that the measured sample purity is independent of the generator top-quark mass value and that the statistical uncertainty on $M_{\rm top}$ covers 68% of the sample measurements. We correct the statistical uncertainty from the likelihood curve using the width of the pull distribution $(M_{\rm top} - m_{\rm gen})/\sigma_{M_{\rm top}}$, where $m_{\rm gen}$ is the generated top-quark mass, $M_{\rm top}$ the measured top-quark mass, and $\sigma_{M_{\rm top}}$ its statistical uncertainty obtained in the pseudo-experiments. The correction factor, 1.17, is independent of the value of $M_{\rm top}$.

The maximum of the one-dimensional top mass likelihood, after correction with the parameterization shown in Fig. 1, corresponds to the value $M_{\rm top} = 177.1 \pm 4.9({\rm stat.})$ GeV/c^2. Figure. 2 shows the corresponding likelihood.

The uncertainty on the JES which varies between approximately 3% and 8% of the measured jet energy, depending on the η and $p_{\rm T}$ of the jet [10], dominates the systematic uncertainties on our measurement of $M_{\rm top}$. We determine its effect using pseudo-experiments in which the JES is increased (decreased) with one standard deviation. Half of the difference in $M_{\rm top}$ between the positive and negative variation of the JES amounts to $\Delta M_{\rm top} = 4.3$ GeV/c^2.

The corrections to $M_{\rm top}$, shown in Fig. 1, depend both on the background fraction and shape. The uncertainty due to the background fraction, varied within the uncertainties of the measured sample purity, is $\Delta M_{\rm top} =$ 1.1 GeV/c^2 for the measured value of $M_{\rm top}$. The relative fractions of the light-flavor QCD background and QCD background containing b quarks is not precisely known. We estimate their ratio (light-flavor/b) to be 2.8 ± 1.0 by performing a binned maximum likelihood fit of the MC expectation to the data based on the jet probability weight distribution in Eq. (2). This result is consistent with a value of 2.7 obtained using the respective QCD cross sections given by the ALPGEN event generator, taking the individual selection efficiencies into account. A systematic uncertainty due to the background composition results in $\Delta M_{\rm top} = 0.8$ GeV/c^2 by varying the background flavor composition between only light-flavor QCD background events and only QCD background containing b quarks.

In accordance with [5], we vary two PYTHIA [18] parton shower parameters, $\Lambda_{\rm QCD}$ and the ISR/FSR transverse momentum scale K-factor, in order to model the systematic uncertainties due to the amount of ISR and FSR. The largest difference observed in $M_{\rm top}$ between any variation amounts to 0.9 GeV/c^2 (0.8 GeV/c^2) for ISR (FSR).

To examine the systematic effect due to uncertainties in the parton distribution function (PDF) of the proton and antiproton, we follow the approach used in [5], resulting in $\Delta M_{\rm top} = 0.8$ GeV/c^2.

By applying the parameterized corrections on $M_{\rm top}$ obtained with HERWIG to MC events generated with PYTHIA we estimate MC modeling uncertainties. The resulting difference in $M_{\rm top}$ equals 0.5 GeV/c^2.

Uncertainties in b-quark fragmentation, semi-leptonic branching ratios, and color-flow affect the b-quark JES [5]. This results in an additional contribution to $\Delta M_{\rm top}$ of 0.5 GeV/c^2. All systematic uncertainties are summarized in Table I. They result in a total systematic uncertainty of $\Delta M_{\rm top} = 4.7$ GeV/c^2.

In summary, we present a new measurement of the top-quark mass in the all-hadronic channel. The measured value is $M_{\rm top} = 177.1 \pm 4.9({\rm stat.}) \pm 4.7({\rm syst.})$ GeV/c^2. This measurement is the first determination of the top-quark mass in the all-hadronic channel using Run II data and is twice as precise as the Run I measurements in this channel [19, 20]. We expect the statistical uncertainty of this measurement to be reduced to 2 GeV/c^2 after analyzing 1 fb^{-1} of integrated luminosity. Our result can be compared with the latest CDF top-quark mass measurements in the dilepton [4] and lepton+jets [5] channel, which are based on samples with a similar integrated luminosity. The measured value for the dilepton chan-

TABLE I: Systematic uncertainties on the measured top-quark mass.

Systematic uncertainty source	$\Delta M_{\rm top}$ [GeV/c^2]
JES	4.3
Background fraction	1.1
Background shape	0.8
ISR	0.9
FSR	0.8
PDF	0.8
MC modeling (generator)	0.5
b-quark JES	0.5
Total	4.7

nel is $M_{\rm top} = 167.9 \pm 5.2(\text{stat.}) \pm 3.7(\text{syst.})$ GeV/c^2, and the value for the lepton+jets channel is $M_{\rm top} = 173.5^{+3.7}_{-3.6}(\text{stat.} + \text{JES}) \pm 1.3(\text{syst.})$ GeV/c^2, where the first uncertainty includes the uncertainty on the jet energy scale, which is measured simultaneously with $M_{\rm top}$. At this level of precision, the values of $M_{\rm top}$ are compatible between all three decay channels.

We thank the Fermilab staff and the technical staffs of the participating institutions for their vital contributions. This work was supported by the U.S. Department of Energy and National Science Foundation; the Italian Istituto Nazionale di Fisica Nucleare; the Ministry of Education, Culture, Sports, Science and Technology of Japan; the Natural Sciences and Engineering Research Council of Canada; the National Science Council of the Republic of China; the Swiss National Science Foundation; the A.P. Sloan Foundation; the Bundesministerium für Bildung und Forschung, Germany; the Korean Science and Engineering Foundation and the Korean Research Foundation; the Particle Physics and Astronomy Research Council and the Royal Society, UK; the Institut National de Physique Nucleaire et Physique des Particules/CNRS; the Russian Foundation for Basic Research; the Comisión Interministerial de Ciencia y Tecnología, Spain; the European Community's Human Potential Programme under contract HPRN-CT-2002-00292; and the Academy of Finland.

[1] The LEP Collaborations, LEP Electroweak Working Group, and SLD Electroweak and Heavy Flavor Groups, Report No. CERN-PH-EP/2005-051, unpublished (2005).

[2] S. Heinemeyer *et al.*, J. High Energy Phys. **09**, 075 (2003).

[3] W-M. Yao *et al.*, J. Phys. G: Nucl. Part. Phys. **33**, 1 (2006).

[4] A. Abulencia *et al.* (CDF Collaboration), Phys. Rev. Lett. **96**, 152002 (2006); A. Abulencia *et al.* (CDF Collaboration), Phys. Rev. D **74**, 032009 (2006).

[5] A. Abulencia *et al.* (CDF Collaboration), Phys. Rev. Lett. **96**, 022004 (2006); A. Abulencia *et al.* (CDF Collaboration), Phys. Rev. D **73**, 032003 (2006).

[6] P. Abreu *et al.* (DELPHI Collaboration), Eur. Phys. J. C **2**, 581 (1998).

[7] D. Acosta *et al.* (CDF Collaboration), Phys. Rev. D **71**, 032001 (2005).

[8] The CDF reference frame uses cylindrical coordinates, where θ and ϕ are the polar and azimuthal angles with respect to the proton beam. The pseudorapidity is defined as $\eta = -\ln\tan\theta/2$, the transverse energy as $E_{\rm T} = E\sin\theta$, and transverse momentum as $p_T = p\sin\theta$.

[9] A. Abulencia *et al.* (CDF Collaboration), Phys. Rev. D **74**, 072005 (2006).

[10] A. Bhatti *et al.*, Nucl. Instrum. Methods A **566**, 375 (2006).

[11] The term light-flavor is used for up, down, strange, and charm flavored quarks or combinations of these.

[12] D. Acosta *et al.* (CDF Collaboration), Phys. Rev. D **71**, 052003 (2005).

[13] A. Abulencia *et al.* (CDF Collaboration), Phys. Rev. D **74**, 072006 (2006).

[14] M. Cacciari *et al.*, J. High Energy Phys. **0404**, 068 (2004); N. Kidonakis, and R. Vogt, Phys. Rev. D **68**, 114014 (2003).

[15] P. Azzi *et al.* (CDF Collaboration), hep-ex/0404010 (2004).

[16] M. L. Mangano, M. Moretti, F. Piccinini, R. Pittau, and A. Polosa, J. High Energy Phys. **07**, 001 (2003); M. L. Mangano, M. Moretti, and R. Pittau, Nucl. Phys. **B 632**, 343 (2002); F. Caravaglios, M. L. Mangano, M. Moretti, and R. Pittau, Nucl. Phys. **B 539**, 215 (1999).

[17] G. Corcella *et al.*, J. High Energy Phys. **01**, 010 (2001).

[18] T. Sjostrand, S. Mrenna, and P. Skands, J. High Energy Phys. **0605**, 026 (2006).

[19] A. Affolder *et al.* (CDF Collaboration), Phys. Rev. D **63**, 032003 (2001).

[20] V. M. Abazov *et al.* (D0 Collaboration), Phys. Lett. B **606**, 25 (2005).